

### Relating forest biomass to TanDEM-X mean phase height

Downloaded from: https://research.chalmers.se, 2025-11-13 22:16 UTC

Citation for the original published paper (version of record):

Askne, J. (2025). Relating forest biomass to TanDEM-X mean phase height. IEEE Journal of Selected Topics in Applied Earth Observations and Remote Sensing, 18: 24039-24050. http://dx.doi.org/10.1109/JSTARS.2025.3606791

N.B. When citing this work, cite the original published paper.

© 2025 IEEE. Personal use of this material is permitted. Permission from IEEE must be obtained for all other uses, in any current or future media, including reprinting/republishing this material for advertising or promotional purposes, or reuse of any copyrighted component of this work in other works.

# Relating Forest Biomass to TanDEM-X Mean Phase Height

Jan I. H. Askne D, Life Fellow, IEEE

Abstract—The Copernicus DEM is derived as a mean of TanDEM-X phase heights. It is known that there is an almost linear-but variable-relationship between phase height and above-ground biomass (AGB). This article investigates the relationship between the mean of TanDEM-X phase heights and AGB. The slope between TanDEM-X phase height and AGB varies across different acquisitions from the same site, influenced by meteorological conditions and the height of ambiguity (HoA), which is the height corresponding to a  $2\pi$  phase shift. An expression based on the Interferometric Water Cloud Model (IWCM) is introduced to represent an average of meteorological variations. This approach uses an ICESat-based method to describe the relationship between area-fill (canopy cover) and forest height. The product of density and height is shown to be approximately linear with AGB under certain conditions. This enables us to express mean phase height as a function of AGB, provided that either the AGB-height allometry or reference AGB values from field data are known. The results demonstrate a strong resemblance and near-linear relationship between mean phase height, mean forest height, and AGB across a wide range of conditions. The analysis is illustrated with 32 TanDEM-X acquisitions from the Remningstorp and Krycklan sites. Forest height and area-fill are estimated from mean phase height, and AGB is also derived for these sites.

Index Terms—Above-ground biomass (AGB), boreal forest, forest height, forest structure, interferometric synthetic aperture radar, TanDEM-X.

### I. INTRODUCTION

BOVE-GROUND biomass (AGB), defined as the density of biomass per unit area (Mg/ha), is a crucial climate variable and one of the 55 Essential Climate Variables (ECVs) of the Global Climate Observing System. It is essential for understanding potential future changes in the climate system [1]. AGB is also closely related to stem (bole) volume (SV), which has economic significance. This underlines the importance of developing biomass retrieval algorithms that relate spaceborne observations to AGB and SV. While stem volume can be estimated using remote sensing techniques, AGB cannot be directly measured by Earth observation due to the inability to detect carbon content and organic mass in woody vegetation. Thus, AGB estimation relies on models.

Important methods for AGB estimation include GEDI (a satellite lidar instrument), CCI, and BIOMASS. CCI uses C-and L-band data that partially penetrate the forest canopy, while

Received 6 June 2025; revised 11 August 2025; accepted 1 September 2025. Date of publication 5 September 2025; date of current version 24 September 2025.

The author is with the Chalmers University of Technology, 412 96 Göteborg, Sweden (e-mail: jan.askne@chalmers.se, jan.askne@gmail.com).

Digital Object Identifier 10.1109/JSTARS.2025.3606791

the BIOMASS satellite employs P-band, which can reach the ground. GEDI, launched aboard the ISS (2018–2019), focused on temperate and tropical forests. BIOMASS targets primarily tropical regions, while C- and L-band data cover most of the globe.

GEDI algorithms predict AGB based on height metrics [2], developed for 32 combinations of plant functional types and world regions. The metric H98 is included in all algorithms, H50 in six, and other percentiles (e.g., H10) in fewer cases. H10 is sensitive to canopy cover but includes ground returns as well.

The CCI method [3] estimates AGB from global C- and L-band backscatter, using ICESat-based relationships between forest height and density. A water cloud model is then used to determine height and its relationship to AGB. This approach is conceptually similar to the one presented in this article.

Different methods provide complementary insights into AGB, each sensitive to different forest characteristics. High-resolution interferometric phase height, which does not suffer from saturation, is a promising method. This study analyses mean values of TanDEM-X phase height, which is also the case for the Copernicus DEM, which is available globally [4]. In addition, a digital terrain model (DTM) is also necessary for estimating phase height, which can be obtained either from BIOMASS in tropical forests or from lidar data in other regions.

Early studies of interferometric phase height in boreal forests date back to the 1990s, when it was discovered that phase height relates to both forest height and area-fill (canopy density), based on three-day repeat-pass ERS-1 C-band observations over northern Sweden [5], [6]. It was noted that such observations could be used to determine the bole volume of the forest [5]. This led to the development of the Interferometric Water Cloud Model (IWCM) [7], [8], which interprets interferometric signals in terms of forest properties such as height, density, and indirectly, SV and AGB, using height-to-AGB relationships or training data. The IWCM has been applied to estimate stem volume from TanDEM-X data [9], [10], [11], [12], including assessments of volume growth [13], forest structure [14], and the potential of C-band bistatic missions [15].

A near-linear relationship between interferometric phase height and AGB was proposed in [16], who found an increase of 14 Mg/ha for each meter of phase height based on two TanDEM-X acquisitions. A similar linear trend was observed in [9], who found variations between 10.3 and 16.4 Mg/ha per meter, with a mean of 13.3 Mg/ha across 18 acquisitions from Remningstorp. This variation reflects the influence of meteorological conditions and HoA.

Many studies have explored the phase height–AGB relationship, from early potential assessments [5] to model-based approaches [18], [19], initial TanDEM-X measurements [9], [16], and more comprehensive observations [20], [21], [22]. Recent work has used the Copernicus DEM minus DTM instead of individual TanDEM-X scenes to estimate AGB in specific areas [23] and across a variety of biomes [24]. This progression raises the question: under what conditions can the mean phase height or the Copernicus DEM be related to AGB?

The IWCM model, which relies on forest height and area-fill, enables the derivation of a relationship between mean phase height (averaged over several acquisitions to minimize meteorological effects) and the product of area-fill and height—and ultimately, AGB. The impact of HoA has then also to be taken into account. Forest height and vegetation ratio are derived from mean phase height, and AGB is estimated using either training areas or AGB-height allometry. The analysis is illustrated using data from the Krycklan and Remningstorp boreal test sites.

Following the dataset descriptions, this article proceeds in two main steps: 1) Exploring the relationship between phase height and the product of forest height and density, based on IWCM, and 2) investigating the relationship between this product and AGB.

### II. TEST SITES

Krycklan (Lat. 64°16′N, Long. 19°46′E) is a river catchment in northern Sweden, covering  $\approx 6800$  hectares of boreal forest. The dominant tree species are Norway spruce (Picea abies), Scots pine (Pinus sylvestris), and birch (Betula spp.). The site has varied topography, with elevations ranging from 145 to 400 m above sea level. It includes mixed ownership and serves as a long-term research area for the Swedish University of Agricultural Sciences (SLU), having hosted the ESA field campaign BIOSAR 2008 [25]. Field and ALS data have supported biomass estimation here.

Remningstorp (Lat. 58°30′N, Long. 13°40′E) is a 1200-hectare estate in the hemi-boreal zone. It features primarily Picea abies, Pinus sylvestris, and Betula spp., with relatively flat terrain (120–145 m elevation). It is also a research site for SLU and was part of ESA's BIOSAR 2010 campaign [26]. Biomass estimation here has been used for both field data and ALS.

Krycklan is a boreal site, whereas Remningstorp is a hemiboreal site. Remningstorp is a well-managed forest site under the Swedish University of Agricultural Sciences (SLU), while Krycklan has many different forest owners with varying management schemes. We have differences concerning climate, ground conditions, meteorological conditions, but also tree species selection, young forest management, rejuvenation methods, timing of when the thinning program starts, etc. (courtesy Ulf Johansson, SLU). The stands at Remningstorp are also smaller compared to those at Krycklan. In this study, we consider 201 stands from Remningstorp, each at least 1 hectare in size, and 241 stands from Krycklan, each at least 4 hectares in size.

### III. ALS DATA

Airborne ALS data from Remningstorp and Krycklan as part of the BIOSAR experiments are used [27], [28]. The ALS

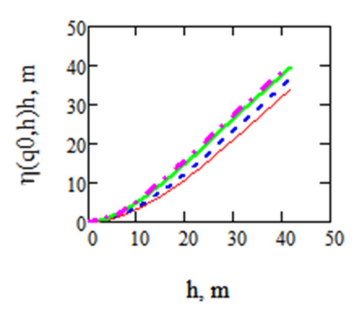


Fig. 1. Relation between  $\eta(q0,h)h$  and h with q0 = 0.04 (red solid), 0.05 (blue dashed), 0.07 (green solid), and 0.08 (red dash-dotted).

observations are trained on extensive in situ observations and we will use the observations of height, H95, the vegetation ratio, VR, and the above ground biomass (AGB) for a number of stands.

The ALS-based height metric H95 is the 95th percentile of lidar returns classified as vegetation returns, i.e., height exceeding 1 m above ground or 10% of the maximum height in a  $10 \text{ m} \times 10 \text{ m}$  grid cell. The vegetation ratio is the proportion of ALS measurements exceeding 1 m above ground or 10% of the maximum height. The AGB, i.e., the mass per unit area in Mg/ha (including stem, bark, branches and leaves/needles, but excluding stump and roots;) is calculated based on biomass functions [26], [28].

### IV. ICESAT DATA

ICESat is a NASA LIDAR satellite for measuring, among other things, vegetation characteristics between 2003 and 2009 with close to global coverage. It has a footprint of 65 m diameter spaced 172 m along track and provides the relationship between canopy density and canopy height, shown to vary across biomes [29] described by a single parameter, q0. The variation in Sweden is investigated in [30].

The area-fill factor in IWCM, corresponding to the ALS vegetation ratio, is expressed as

$$\eta(q0,h) = 1 - e^{(-q0h)}.$$
(1)

In this article, the product  $\eta(q0,h)h$  will be of particular interest, and the variation for a change of q0 as illustrated in Fig. 1.

### V. TANDEM-X DATA

For Remningstorp, 18 TanDEM-X acquisitions from June 2011 to August 2012 are studied, with heights of ambiguity varying from 49 to 358 m [9]. For Krycklan, 14 TanDEM-X acquisitions from June 2011 to August 2014 are studied, with HoA ranging between 36 and 135 m [11], [13]. Two acquisitions from Krycklan were acquired during winter conditions. We will use phase-height information from all 32 TanDEM-X acquisitions, see Appendix A.

Although we here concentrate on TanDEM-X data a goal is to investigate the possibility to use Copernicus DEM for AGB estimation, since Copernicus DEM is available worldwide and based on a mean of a few TanDEM-X acquisitions with heights of ambiguity somewhat related to the canopy height and with a goal to be independent of meteorological variations.

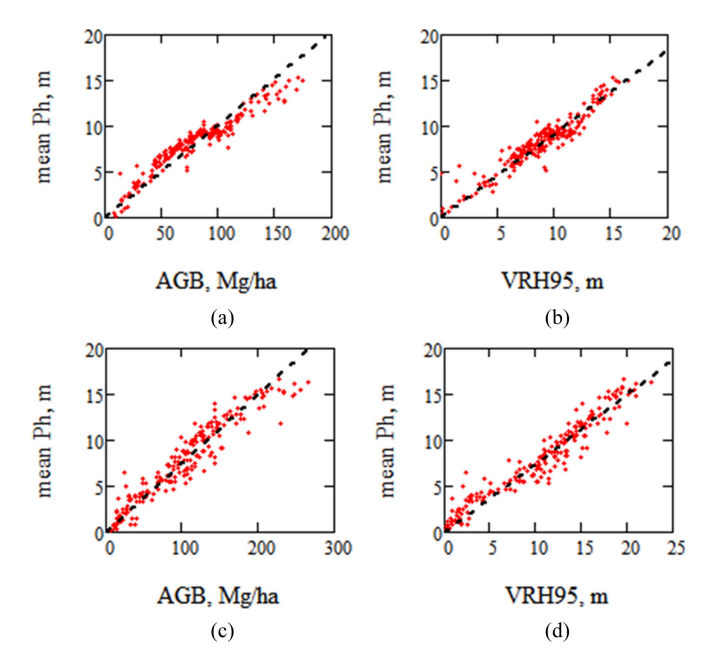


Fig. 2. Illustrating (a) mean phase height versus AGB and (b) versus vegetation ratio times height in Krycklan and (c) and (d) the same for Remningstorp.

TABLE I SLOPE COEFFICIENTS AND PEARSON'S R2

Site	κ <sub>1</sub>	r1 <sup>2</sup>	κ <sub>0</sub>	r2 <sup>2</sup>
Krycklan	9.83	0.906	0.92	0.895
Remningstorp	13.33	0.906	0.75	0.928

meanPh versus AGB is denoted r1<sup>2</sup> and meanPh versus VR.H95 is denoted r2<sup>2</sup>.

### VI. OBSERVATIONAL RESULTS FROM KRYCKLAN AND REMNINGSTORP

### A. Mean TanDEM-X Phase Height

The TanDEM-X phase height, Ph, is dependent on the meteorological influence on attenuation and backscatter as well as by the height of ambiguity (HoA) of which only HoA is known. By averaging TanDEM-X acquisitions the meteorological influence can be reduced. Fig. 2 shows the mean of 14 TanDEM-X acquisitions from Krycklan and 18 from Remningstorp versus AGB, and versus the product of vegetation ratio, VR, and H95.

For these almost linear relations, the slope for meanPh versus AGB and meanPh versus VR·H95 have been determined by minimization of the sum of the quadratic difference between the stand values as  $\kappa_1$ ·meanPh = AGB and meanPh =  $\kappa_0$ ·VR·H95, see Table I.

Pearson's  $r^2$  (also denoted  $r^2$ ) are high, and we conclude there are strong, and almost linear, relations between meanPh, VR·H95, and AGB.

### B. Individual TanDEM-X Phase Height Observations

The mean TanDEM-X phase height is based on a number of individual observations for which the variability will be illustrated. The relations  $Ph = \kappa_0 VR \cdot H95$  and  $\kappa_1 \cdot Ph = AGB$  are determined as above, and the parameters are illustrated in Fig. 3.

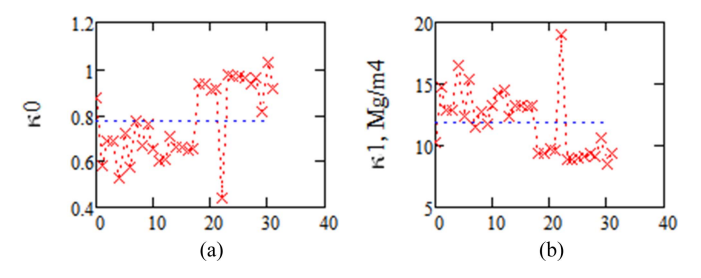


Fig. 3. Illustrating in (a)  $\kappa_0$ , and in (b)  $\kappa_1$  for 18 observations from Remningstorp followed by 14 from Krycklan, see Appendix A for numbering. Dotted blue lines represent mean values of 0.77 and 11.82.

 $\kappa_0$ , and  $\kappa_1$  have a standard deviation of 0.16, assumed to be related to meteorological variations, forest properties, and HoA variations. The anomalous behavior of one observation from Krycklan is when the temperature is -10 °C. We also see that the Remningstorp values are more variable than those from Krycklan. From this, we conclude that there is a relatively large variability of the individual TanDEM-X phase height, and we need an expression for the mean phase height independent of meteorological variations and sites, which can take this into account.

### VII. INTERFEROMETRIC WATER CLOUD MODEL

IWCM was introduced in [7] and applied to a larger area in [8]. The model has been described in several papers, most recently in [15]. IWCM is based on a simple model consisting of a layer of randomly scattering particles concentrated to a fraction,  $\eta$ , of the unit area.  $\eta$  is called the area-fill. IWCM describes the forest horizontally by the area-fill  $\eta$ , and vertically by the height, h. The vegetation with its gaps is in practice distributed stochastically over the area.

In the fraction  $\eta$  of the unit area with scatterers the microwaves are reaching ground after attenuation by  $\alpha$ , Np/m, back and forth, while in the rest of the area (the gaps within or between trees), the microwaves are reaching ground without any attenuation. The backscattering from the forest layer is described by  $\sigma_{\rm veg}^0$  and from the ground by  $\sigma_{\rm gr}^0$ , the latter depends on, e.g., roughness, dielectric properties and moisture. The model is most relevant for C- and X-band while lower frequencies penetrate more into the forest layer, which may lead to more complex interactions e.g., ground-stem scattering. The backscatter part of the model has been successfully used in the BIOMASAR approach, which estimates AGB from a time series of SAR backscatter observations [3], [31], [32] in order to eliminate meteorological influence.

According to the model we may consider  $\eta h$  a measure of the mean height. Knapp et al. [33] found that the mean canopy height was the most important predictor variable for biomass estimation from lidar across forest types from different continents including temperate and tropical forests. In their case the mean height is defined as the mean of all the lidar point clouds rasterized with 1-m resolution. In [34], it was found that H50 was better characterizing AGB than top of canopy height.

Based on TanDEM-X observations of phase height, coherence and backscatter, using a known DTM and allometric relations between the area-fill and height,  $\eta(h)$ , and AGB and height,

AGB(*h*), the forest density, height and AGB can be estimated from IWCM e.g., [15], without training samples, based on the constraints of observed backscatter, coherence and phase-height. However, here we will only use mean phase height. The validation of the model is based on the accuracy of the model estimates compared to ALS or in situ observations [9], [11], [13], [14].

### A. Area-Fill Allometry

Area-fill is the fraction of the area for which the phase front is affected by dielectric attenuation, etc. Different approaches to express the allometry have been used, see Appendix B, first an approach where the backscatter was estimated to vary as  $\exp(-\beta V)$  [35]. The  $\beta$ -approach was used for TanDEM-X acquisitions [9], and  $\beta$  varied slightly for different acquisitions based on training stands. Later, an area-fill based on the vegetation ratio for the test sites was used, and a solution method without training samples [10]. We will now use a simple one-parameter expression for the canopy density,  $\eta(q0,h) = 1 - e^{-q0 \cdot h}$ , which is the expression used in the interpretation of ICESat GLAS observations for the observed density-height relation [29]. It has been used for Swedish conditions together with the extended Water Cloud Model (backscatter part of IWCM) to estimate AGB [30] and world-wide in [3]. The accuracy of the expression is limited by its simplicity, but this can partly be compensated for in IWCM by means of adjusting the parameters  $\alpha$  and m such that the expression for phase height is adjusted to the observations. From a map of q0-values in Sweden [30], we have chosen q0 =0.055 for Krycklan and 0.065 for Remningstorp.

### B. AGB Allometry

In IWCM, forest height is the variable that can be observed, and to obtain AGB, we need a relation between the two. AGB is often related to height in the form

$$AGB = a \cdot h^b \tag{2}$$

where b can be denoted the height-biomass exponent. Estimated parameters a and b differ across forests, see e.g., [36]. A value close to 2 for b was found in [37] for forests on three continents. In [3], b was found to vary between 1.4 and 2.3, but in Sweden, based on National Forest Inventory, NFI, plots [30], b was determined to a mean of 2.6 with relatively large variations over the country.

Investigations indicate that the main error of a height-biomass allometry is the missing information of forest density or basal area, see e.g., [38]. In Fig. 4, we illustrate the relation between H95 and AGB and  $VR \cdot H95$  and AGB for the two sites.

 $\eta(q0,h) \cdot h$  is the model expression for VR·H95, but including a factor 0.95 and 0.90 for an allometric relation after minimizing the quadratic difference with AGB(H95). (It can be remarked that choosing q0=0.05 for both sites would give a good agreement without extra factors in both cases, however, we will use q0-factors as estimated from [30].

We may now either express AGB with a and b as  $ah^b$  or with  $\kappa_b$  (biomass coefficient) and q0 as  $\kappa_b \cdot \eta(q0, H95) \cdot H95$  or relate AGB to the product of VR and H95, see Tables II and III.

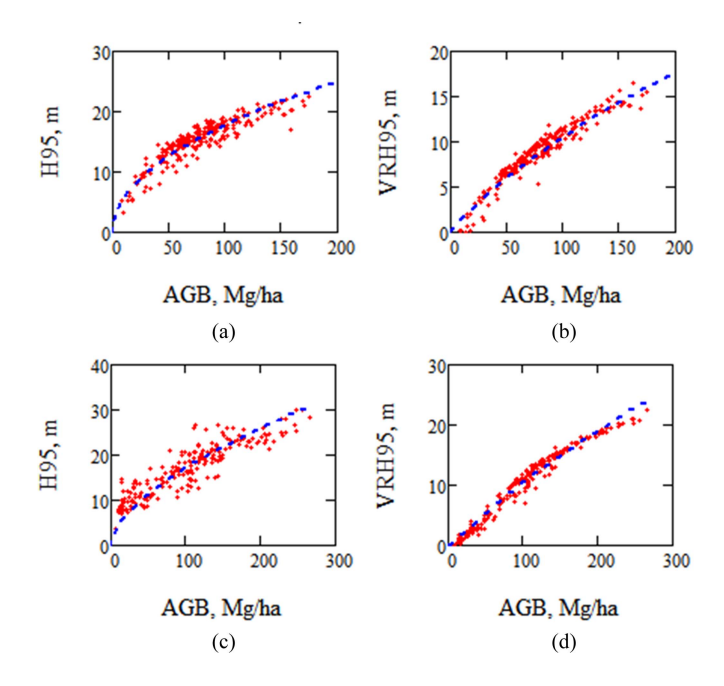


Fig. 4. (a) and (b) ALS data and allometry for Krycklan. (a) H95 versus AGB and allometric relation AGB(h) (blue dotted line), (b) VR·H95 versus AGB and  $0.95\eta(q0,h)\cdot h$  versus AGB(h), (c) and (d) for Remningstorp: (c) H95 versus AGB and allometric relation AGB(h) (blue dotted line), (d) VR·H95 versus AGB and  $0.90\eta(q0,h)\cdot h$  versus AGB(h). For AGB(h), see Table II.

TABLE II RESULTS FROM ESTIMATION OF AGB AS AGB(H).

Site	а	b	RMSEr	r2
Krycklan	0.280	2.041	16.8	0.85
Remningstorp	0.814	1,689	25.9	0.81

TABLE III RESULTS FROM ESTIMATION OF AGB AS  $\kappa \text{B2-VR-H95}$  and as  $\kappa \text{B-}\eta(\varrho 0,\text{H95})$  . H95

Site	κb2	RMSEr	r2	κb	RMSEr	r2
Krycklan	9.116	13.5	0.91	9.057	18.4	0.83
Remnings-	10.132	12.8	0.95	9.278	26.3	0.81
torp						

The a and b-values for Krycklan and Remningstorp differ, but the  $ah^b$  expressions are very similar. The best accuracy for AGB is when expressed as  $\kappa b \cdot VR \cdot H95$ , the next best as  $ah^b$  and finally  $\kappa b \cdot \eta(q0,H95) \cdot H95$ , probably due to the relatively approximate expression for the area-fill. It is well known that AGB is accurately expressed by the product of basal area and height, and a relation between VR and basal area, based on data from Krycklan, is investigated in Appendix C.

### C. IWCM Expression for TanDEM-X Phase Height

The IWCM expression for phase height, see e.g., [15], is depending on the volume decorrelation and the backscatter from ground relative the vegetation. The volume decorrelation is a basic quantity in SAR interferometry and can be related to the forest height and the attenuation coefficient  $\alpha$  by the following

expression, see e.g., [7], [15]

$$\begin{split} \tilde{\gamma}_{\text{vol}} &= \frac{\int_0^h e^{-\alpha(h-z')} \cdot e^{-j\frac{2\pi}{\text{HoA}}z'} \text{d}z'}{\int_0^h e^{-\alpha(h-z')} \text{d}z'} \\ &= \frac{\alpha}{\alpha - j\frac{2\pi}{\text{HoA}}} \left( e^{-j\frac{2\pi}{\text{HoA}}h} - e^{-\alpha h} \right) \frac{1}{1 - e^{-\alpha h}} = \gamma_{\text{vol}} e^{-j\varphi}. \end{split}$$

The volume decorrelation is only part of the complex phase expression, which is also related to the ground versus vegetation backscatter, m,

$$\hat{\gamma} = \gamma_{sys} \frac{\tilde{\gamma}_{\text{vol}} + M}{1 + M} \text{ where } M = m \frac{\frac{1 - \eta}{\eta} + e^{-\alpha h}}{1 - e^{-\alpha h}} \text{ and } m = \frac{\sigma_{gr}^0}{\sigma_{\text{veg}}^0}.$$
(4)

Phase height can finally be expressed as, see Appendix D, when the ground phase is compensated by a known DTM

PhIWCM = 
$$-\frac{\text{HoA}}{2\pi} \arg(\hat{\gamma})$$
  
=  $-\frac{\text{HoA}}{2\pi} \left[ \varphi - \operatorname{atan} \left( \frac{\sin(\varphi)}{\frac{\gamma_{\text{vol}}}{M} + \cos(\varphi)} \right) + n \cdot 2\pi \right].$  (5)

The minus sign is related to the  $\exp(-j\frac{2\pi}{\text{HoA}}z)$ -assumption, and n to the possible phase shifts. PhIWCM is a function of  $\alpha$ , m, HoA and n, where n is the branch of solutions.

When  $2\pi/\alpha \text{HoA} \ll 1$  and  $\exp(-\alpha h) << 1$ , we obtain from PhIWCM, see Appendix D, with two alternative approximate relations

$$Ph \approx \eta \frac{h - \frac{1}{\alpha}}{\eta + m (1 - \eta)}$$

$$\approx \begin{cases} \eta \left( h - \frac{1}{\alpha} \right) & \left( \frac{2\pi}{\alpha \text{HoA}} \ll 1, e^{-\alpha h} \ll 1 \right). \end{cases} (6)$$

The approximation  $\eta(q0,h)\cdot(h-1/\alpha)$  [14], is based on a simple view of the model with a phase height  $h-1/\alpha$  from  $\eta$  of the area and zero elsewhere, and can be obtained from (6) if we use m=1 (m can be larger or smaller than 1). When h is large,  $\eta$  is close to one and Ph tends to h-1/ $\alpha_{\rm eff}$ , where  $\alpha_{\rm eff}$  is a slight correction of  $\alpha$ , [9].  $\eta h$  represents the mean height in IWCM and the mean height is often a good estimate of AGB.  $\kappa_0$  is a variable part, investigated below and related to the electromagnetic scattering process. This means that the phase height under simplified conditions can be seen as the forest height corrected by a penetration depth taking the canopy density into account.

With the approximate expression, it is easier to discuss the sensitivity of phase height to the parameters. We see that the phase height is increasing if the attenuation in the vegetation layer is increasing (e.g., the penetration depth is decreasing) and if  $m = \sigma_{gr}^0 / \sigma_{veg}^0$  is decreasing. There is a meteorological dependence of the phase height through  $\alpha$  and m, but also a dependence on forest structure through  $\eta(q0,h)$  and h. m is in Krycklan typically below or around 1 and for Remningstorp around 1 or larger, [9], [13].

Finally, it should be noted that h is a proxy in IWCM for H95 or for Lorey's height (basal area weighted mean height)

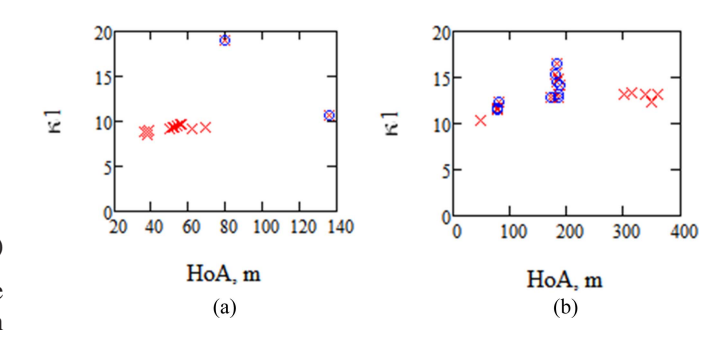


Fig. 5. Illustrating  $\kappa_1$  versus HoA for (a) Krycklan and (b) Remningstorp. Acquisitions from winter months are marked by blue circles.

when comparing h with in situ data.  $\eta(q0,h)$  is a proxy for vegetation ratio, VR, when comparing with ALS data. In practice the ICESat expression  $\eta(q0,h)$  is a rather approximate proxy for VR in particular for lower values of height, see Appendix C.

#### D. TanDEM-X Observations Versus HoA

When HoA is large, the measurement uncertainty increases. However, when HoA is relatively small, e.g., 50 m, there is a phase height transition when the phase height reaches  $\approx$ HoA/2, which influences the observations, particularly if this is within the heights of the forest. For the 14 observations from Krycklan and 18 from Remningstorp HoA is in the range 36–136 m for Krycklan and 49–359 for Remningstorp, see Fig. 5, but the influence on the phase height is mainly when HoA is low.

We see a higher variability of  $\kappa_1$  (the slope between phase height and AGB) for winter conditions (December–April) with risks for wet snow or below zero degrees, and a slight trend for lower  $\kappa_1$  for lower HoA, while the summer acquisitions are relatively stable. The winter temperatures are lower for Krycklan than Remningstorp and for one acquisition in Krycklan when HoA is 79.4 m, the temperature is -10 °C associated with a very low phase height. We also note the generally lower values of  $\kappa_1$  for Krycklan compared to Remningstorp correlated to lower  $\sigma_{\rm gr}/\sigma_{\rm veg}$  in Krycklan compared to Remningstorp [9], [11] and possibly related to ground moisture and also to forest structure.

### E. IWCM Mean Expression

We have obtained an explicit expression for IWCM phase height and its sensitivity to  $\alpha$ , m, and HoA. With Monte Carlo simulations, we will now investigate the range of variations. In Fig. 6, we illustrate the variation of the phase height for uniformly distributed random numbers between 0.1 and 0.5 for  $\alpha$  and 0.4 and 2 for m, which represent the observed variations. As a mean expression for the phase height, according to Fig. 6, we introduce, based on the simulations, Phmean(HoA,h,n)

Phmean (HoA, 
$$h, n$$
) 
$$= \text{PhIWCM} (\alpha = 0.17, m = 1, \text{HoA}, h, n). \tag{7}$$

The left figures in Fig. 6 illustrates the range of variation when HoA = 80 and the results are similar for HoA > 80, while the right figures are for HoA = 40 and for HoA < 40 the variability around and the deviation from the dashed equal-line is still more pronounced below Ph = HoA/2. The approximation

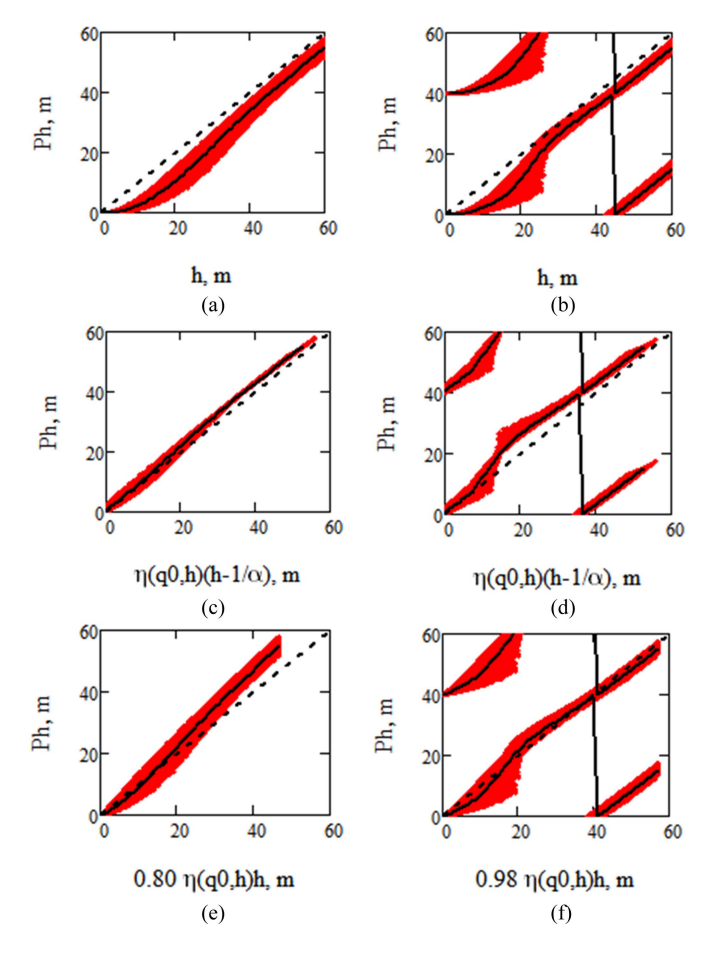


Fig. 6. Illustration of IWCM phase height as a function of height, and the two approximative expressions of phase height from  $10^5$  Monte Carlo simulations with  $0.1 \le \alpha \le 0.5$  and  $0.4 \le m \le 2$  (red dots) and Phmean (black line) with  $\alpha = 0.17$  and m = 1. The figures (a), (c), and (e) illustrate HoA = 80 m, and (b), (d), and (f) HoA = 40 m with associated branches when h and Ph > HoA.  $\kappa_0$  is in (e) 0.8 and in (f) 0.98.

 $\eta(q0,h)(h-1/0.17)$  is very good when HoA  $\geq$  80. With HoA = 40, the illustrated spread of the phase height when Ph < HoA/2 increases and the uncertainties in Phmean increases.

Fig. 6(e) shows that  $0.8\eta(q0,h)h$  is an adequate approximation for heights up to  $\approx 25$  m, while Fig. 6(f) shows that  $0.98\eta(q0,h)h$  is a good approximation for larger heights, even up to 60 m, i.e., tropical conditions, and for these heights the spread is small when HoA = 40 m as well as 80 m, i.e., the mean phase height is closely related to  $\eta(q0,h)h$ , the mean height according to the model, and  $\eta(q0,h)h$  is closely related to AGB.

### VIII. FROM MEAN PHASE HEIGHT TO FOREST PROPERTIES: HEIGHT AND VEGETATION RATIO

We have now studied the variability of phase height due to meteorological conditions and HoA, but we have also illustrated the stability of the mean of several acquisitions and identified expressions,  $0.8\eta(q0.h)h$  and Phmean, for the mean phase height dependence on height for boreal forests, expressions that now can be used to estimate height and vegetation ratio for the boreal sites of interest. We will study Phmean for all observations as

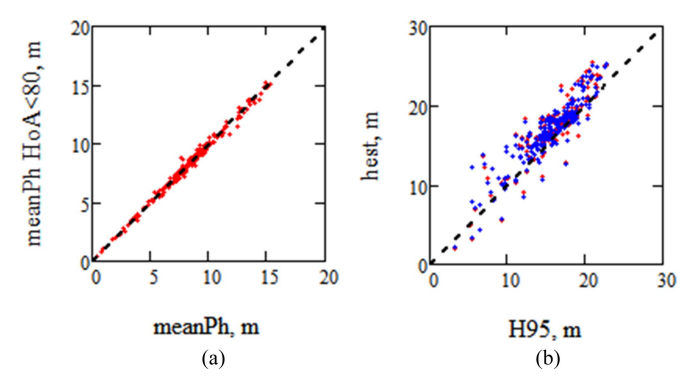


Fig. 7. (a) Illustrating the mean phase height, for those 13 with HoA<80 versus all 14 acquisitions from Krycklan, and (b) the corresponding estimated heights versus H95 from meanPh =  $0.8 \cdot \eta(q0,h) \cdot h$ , red dots based on meanPh for all and blue dots from those 13 with HoA<80 m.

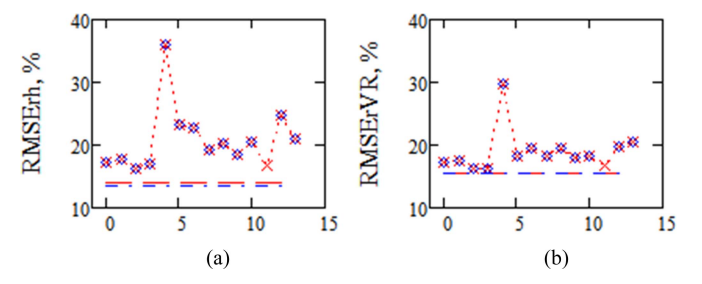


Fig. 8. Illustrating RMSEr for Krycklan estimated (a) height, and (b) vegetation ratio, for each of the acquisitions (red cross) and those with HoA<80 (blue circles). Red dashed line indicates the RMSEr based on mean phase height for all acquisitions and blue dash-dotted line for those with HoA<80.

well as for those with HoA<80 m since HoA affects the phase height expression for lower heights when HoA is low and the Copernicus DEM can be expected to be based on observations with HoA<80 for the boreal area with typical forest heights.

In Krycklan, 13 out of 14 acquisitions have HoA<80 m. With phase height < HoA/2 we interpret the phase height as  $0.8 \cdot \eta(q0,h) \cdot h$  independent of HoA and obtain estimates of the heights,  $h_{\rm est}$ , by identifying the expression with the observed phase heights, see Fig. 7(b).

We also determine the accuracy of estimated heights and estimated vegetation ratio  $\eta(q0,h_{\rm est})$  in the form of RMSEr relative in situ observations, for each of the 14 acquisitions as well as those 13 acquisitions with HoA<80 m, see Fig. 8. The results for those 13 with HoA below 80 m compared to all 14 acquisitions agree quite well with all, as expected.

The RMSEr is particularly high for the case when temperature is -10 °C, see Fig. 8, when the phase height is extra low. Finally, we see that the RMSEr of the mean phase height groups (all 14 or 13 with HoA <80 m) seems to be close to the best estimates of the individual acquisitions.

In Remningstorp, HoA values extend up to 359 m, but four out of 18 acquisitions have HoA<80 m and are affected most by HoA. Those four are illustrated relative to all the phase heights in Fig. 9(a). We interpret the mean phase height as  $0.8 \cdot \eta(q0,h)$ .

From Fig. 9, we see a slope difference between those with HoA<80 and since Copernicus DEM is based on acquisitions

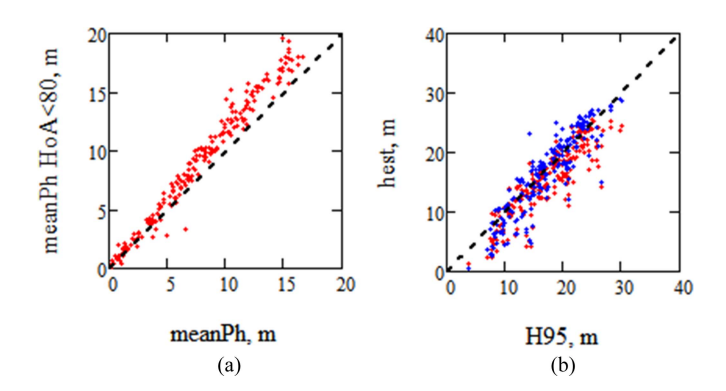


Fig. 9. (a) Illustrating meanPh =  $0.8 \cdot \eta(q0,h) \cdot h$  for those four with HoA<80 versus all 18 acquisitions from Remningstorp, and (b) corresponding estimated heights versus H95, red dots based on meanPh for all, and blue dots for those four with HoA<80 m.

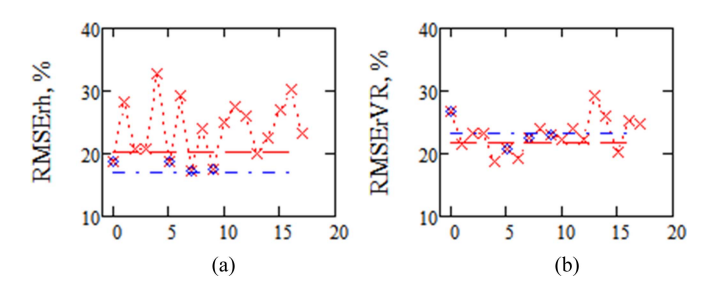


Fig. 10. Illustrating RMSEr for Remningstorp estimated (a) height, and (b) vegetation ratio, for each of the acquisitions (red cross) and those with HoA<80 (blue circles). Red dashed line indicates the RMSEr based on mean phase height for all and blue dash-dotted line for those with HoA < 80 m.

TABLE IV
PARAMETERS DERIVED FOR KRYCKLAN FROM MEANPH AND PHIWCM AND A
TENTH OF THE AGB VALUES IN THE AREA, ESTIMATED RMSER FOR TESTING
STANDS AND MEAN PHASE HEIGHT OF 14 ACQUISITIONS

Model	$\alpha_{\text{eff}}$	m <sub>eff</sub>	RMSErh %	а	b	RMSErB %
0.8η(q0,h)h	_	_	12.42	0.14	2.22	11.15
PhIWCM	0.08	0.09	9.84	0.12	2.34	12.46

q0 = 0.055, HOAm = 58.29 m for PhIWCM.

with relatively low HoA, we analyze separately the four acquisitions with HoA < 80 and find that the slope versus AGB is 11.45 instead of 13.33 for all and RMSEr of estimated AGB 16.7% instead of 18.1% related to the higher phase accuracy with lower HoA. This means that the Remningstorp slope value in this case is closer to the one for Krycklan, cf. Table I.

We also determine the accuracy of estimated heights and estimated vegetation ratio, in the form of RMSEr relative in situ observations, from each of the 18 acquisitions as well as those four acquisitions with HoA<80 m, see Fig. 10. The results for those four with HoA below 80 m compared to all 18 acquisitions now differ related to HoA. The improvement in RMSEr when using the mean phase heights is more obvious in Krycklan, which is assumed to be related to the approximate expression for the mean phase height. In Tables IV and V, below, the results from using Phmean will be listed for Krycklan and Remningstorp.

#### TABLE V

Parameters Derived for Remningstorp From Meanph and PhIWCM and a Tenth of the AGB Values in the Area, Estimated RMSEr for Testing Stands and Mean Phase Height of 18 Acquisitions,  $\varrho 0=0.065$ , HOAm=199.3 m, as Well as Those With HoA<80 m

Model	$\alpha_{\text{eff}}$	m <sub>eff</sub>	RMSErh	а	b	RMSErB
			%			%
0.8η(q0,h)h	_	_	19.97	0.63	1.74	17.95
PhIWCM	0.24	0.8	16.94	0.32	1.98	17.96
0.8η(q0,h)h	_	_	16.96	0.84	1.68	16.44
PhIWCM	0.12	0.52	15.49	0.32	1.99	16.47

With HOAm = 71.7 m for PhIWCM.

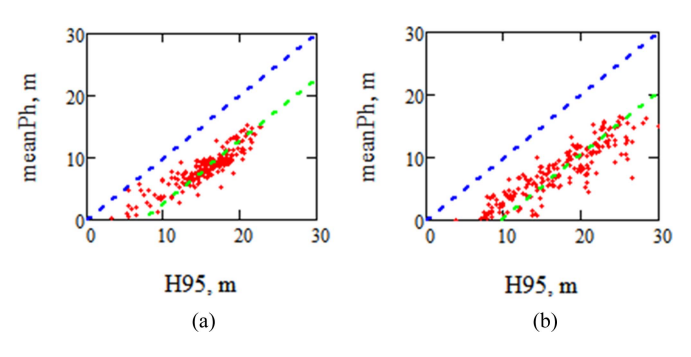


Fig. 11. Illustrating meanPh versus H95 for (a) Krycklan and (b) Remningstorp. A line, 7.2 m below the diagonal, in the case of Krycklan, and 9.5 m, in the case of Remningstorp, is included.

### IX. PENETRATION DEPTH

The importance of the penetration depth is often discussed related to TanDEM-X phase height [39], since this penetration affects the height and AGB retrieval and then may be corrected in a first stage. As illustrated in (5), the phase height is strongly related to the volume decorrelation and then  $\alpha$  and HoA, but also to  $\sigma_{\rm gr}^0/\sigma_{\rm veg}^0$  and to the vegetation density, which complicates. The penetration depth in the data from Krycklan and Remningstorp is illustrated in Fig. 11. The penetration depth is not an important parameter in this analysis.

### X. NEED FOR REFERENCE AREAS

A common method in remote sensing based on a model or on statistical methods is to use reference stands to relate model parameters to AGB. For simplicity, we illustrate the method by using 10% of the available stands for training and the rest for testing (only a small number of stands should be considered known). The stands are ordered after increasing AGB and each tenth stand is chosen as a training stand, giving a range of stands covering the range of AGB values.

For Krycklan and Remningstorp, we first used meanPh  $= 0.8\eta(q0,h)h$  from which  $h_{\rm est}$  is determined. We then replace h by (2), i.e.,  $h = h(a,b,{\rm AGB})$  and obtain a relation meanPh $(a,b,{\rm AGB})$ . With known reference AGB values, we minimize the quadratic difference, F(a,b), between the model and the known observations to obtain a and b. With those values and  $h_{\rm est}$ , we can determine AGB for the test area

$$F(a,b) = \sum (\text{meanPh}(a,b,AGB) - \text{Ph})^{2}.$$
 (8)

Similarly, with known reference values for H95, we can minimize the quadratic difference between the model and the observations and obtain  $\alpha_{\text{eff}}$  and  $m_{\text{eff}}$ , using a mean value of HoA, HoAm, for the involved acquisitions (n = 0 for Krycklan and Remningstorp)

$$F2\left(\alpha_{\rm eff}, m_{\rm eff}\right) = \sum \left(\text{PhIWCM}\left(\text{HoA}m, \alpha_{\rm eff}, m_{\rm eff}, H95\right) - \text{Ph}\right)^{2}. \tag{9}$$

The summation takes place over the training stands with known H95. With  $\alpha_{\rm eff}$  and  $m_{\rm eff}$ , we can determine an effective expression for PhIWCM and then also check how well the simple  $0.8\eta(q0,h)h$  agrees and decide if the inversion process can be improved.

The results for Krycklan are given in Table IV. With meanPh expressed as  $0.8\eta q0,h)h$ , we estimate h and RMSErh, and with known AGB for the training stands we estimate a, b, AGB(h), and RMSErB for AGB. With H95 for training stands, we estimate  $\alpha_{\rm eff}$  and  $m_{\rm eff}$  in (9) and an improved value of RMSErh, while the AGB estimation is slightly worse than the first approach.

The corresponding results for Remningstorp are given in Table V. Of 18 TanDEM-X acquisitions, only four have HoA < 80. We have then investigated separately results based on the four cases with meanPh determined from those with HoA < 80 m.

The values of  $\alpha_{\rm eff}$  and  $m_{\rm eff}$  have lost much of their physical significance since they are based on the mean phase height of 14 and 18 acquisitions, respectively, with different HoA.

The results are illustrated in Fig. 12.

### XI. EXTENSION OF AGB RELATION

In this article, the mean phase height was first related to  $\eta(q0,h)h$  and then  $\eta(q0,h)h$  was related to AGB. The latter step can be seen to be in line with the basal area times height is proportional to stem volume and AGB, cf. Appendix C. On the other hand, AGB has also been expressed in the more conventional manner as  $AGB(h) = ah^b$ . In Sweden, it has been found, by studies of NFI plots, that the AGB expression of the type (2) varies considerably [30], resulting in a mean height-biomass exponent b = 2.613 for AGB up to approximately 260 Mg/ha (stem volumes 800 m<sup>3</sup>/h). However, the height dependence of the expression  $\eta(q0,h)h$  is limited by the range of q0-values, in Sweden between 0.05 and 0.08 with a mean of 0.061 [30] and generally between 0.02 and 0.16 [29]. This will limit the AGB dependence on h as expressed by  $\eta(q0,h)h$ , and it can be assumed that the relation between area-fill and basal area is more nonlinear for the higher values of b.

For this reason, the variation of the Phmean-expression in (7), as well as  $\eta(q0,h)h$ , will be investigated relative AGB expressions of the type  $ah^b$  for a range of b-values in Fig. 13, where the a-coefficient is chosen such that 13.3 Phmean  $\approx$  AGB. We see that Phmean is approx. proportional to AGB when HoA = 80 m, but more nonlinear with AGB if HoA = 40 m.  $\kappa 0 \cdot \eta(q0,h)h$  is most linear with AGB for the two lower values of b.

This illustrates limitations in the link from Phmean via  $\eta(q0,h)h$  to AGB. Nevertheless, we see that Phmean has a linear relation to AGB over a large range of biomass-coefficients,

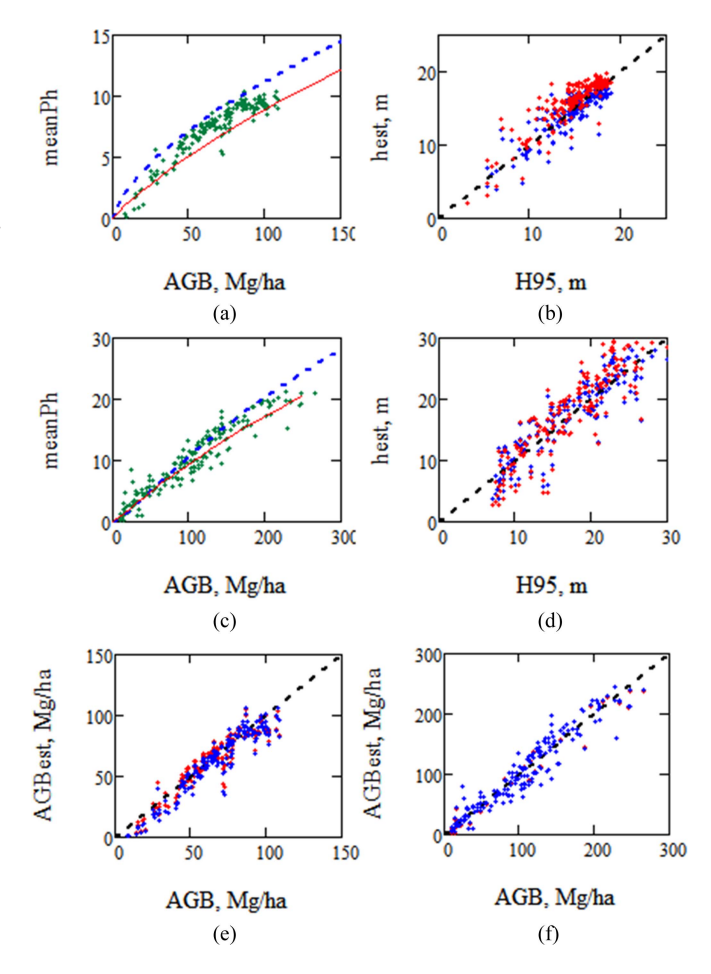


Fig. 12. (a), (b), and (e) for Krycklan with mean HoA = 52.32 m, (c), (d), and (f) for Remningstorp with mean HoA = 71.54 m. (a) and (c) meanPh versus AGB in green dots together with model  $0.8\eta$  (q0,h)h in red line, and model PhEx( $\alpha$ ,m,HoAm,0) with H95 for training stands known in dotted blue line. (b) and (d)  $h_{\rm est}$  and (e) and (f) AGB<sub>est</sub> illustrated in red based on model  $0.8\eta$  (q0,h)h in red dots and with H95 from training stands in blue dots (in f the red and blue dots are almost overlapping).

which is the important point in our investigation of the relation between biomass and mean phase height. The relation between  $\kappa 0\eta(q0,h)h$  and AGB is relatively linear for b-values up to 2.6, which indicates that the q0 values together with maximum forest height, both possible to determine with satellite, still have a guiding value in identifying areas with similarities and facilitate the choice of training sites.

### XII. DISCUSSION

The assumption that phase height depends on both height and density dates back to [5], with the IWCM model introduced [7] to account for this relationship. However, the lack of satellite density information posed a complication that was eventually resolved using data from ICESat [24]. A solution to IWCM, incorporating constraints from phase height, coherence, and backscatter, without relying on training samples, was presented by [11]. The studies in [23] and [24], which demonstrate a relationship between the World DEM and AGB, required a solution based solely on phase height.

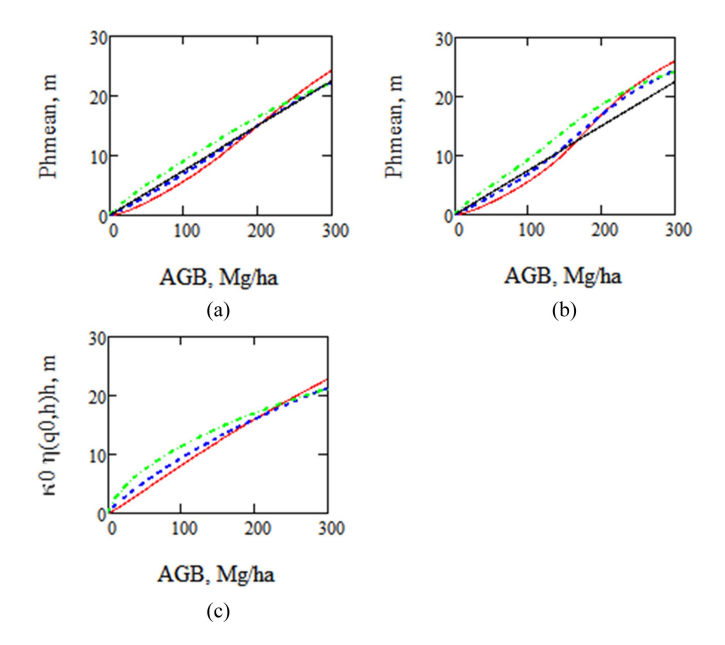


Fig. 13. Phmean and  $\kappa 0 \eta(q0,h)h$  with  $\kappa 0=0.8$  and q0=0.06 illustrated versus AGB(h) =  $ah^b$  in three cases AGB(h) =  $1.33h^{1.6}$ , (red line), AGB(h) =  $0.38h^{2.0}$ , (blue dotted), and AGB(h) =  $0.052h^{2.6}$ , green dotted). In (a) and (b) the black solid line represents 13.3Phmean = AGB. For (a) Phmean with HoA = 80 m, (b) Phmean HoA = 40 m, and (c)  $\kappa 0 \eta(q0,h)h$ .

It is known that there is an almost linear relation between X-band phase height and biomass [9], [16], [40]. However, it has also been shown that this slope is varying between different acquisitions [9]. In [24], it was found that several investigated sites showed a relatively constant proportionality between the Copernicus DEM–DTM on one hand and AGB on the other, and also with lower scattering of the data points than other presently used satellite methods to estimate AGB. Since Copernicus DEM is formed as the mean of several suitable TanDEM-X phase heights it brings up the question of the relation between mean values of TanDEM-X phase heights and AGB.

The variability in the slope between phase height and AGB is determined by the meteorological effects on the attenuation and scattering of the microwaves in the forest, and it seems natural to focus on averaging the phase heights from a number of TanDEM-X acquisitions and to study properties of such averages. An average of the results in [9] derived from each acquisition weighted by HoA was earlier derived for Remningstorp with an AGB accuracy of 16.5% using half of the stands, at least 1 ha large, for training and half for testing based on knowledge of coherence and backscatter as well as phase height. With only information on the phase height, a mean value must be formed in another manner, and by Monte Carlo simulated variations, a mean over typical properties could be formed.

Since there is no direct physical link between InSAR phase height and AGB, instead we have focused on the product of vegetation ratio and height as an intermediate product. By means of the relation between area-fill and height, based on ICESat GLAS measurements [29], [30],  $\eta(q_0,h)$ , and with expressions for the IWCM phase-height, it was shown that the mean phase height, under some relatively general conditions, can be expressed in  $\eta(q_0,h)\cdot h$ , where  $q_0$  is an ICESat GLAS determined quantity

and h is the height of the forest layer.  $\eta(q_0,h)\cdot h$ , which is an IWCM expression for the mean forest height, is shown to have an approximately linear relation to AGB(h) =  $a\cdot h^b$  for a large range of b-values. With AGB values available from reference areas, the a and b values can be estimated from the mean phase height. Alternatively, if a and b are known for the type of area an expression meanPh(HoA,  $q_0$ , a, b, AGB), where  $q_0$  and a mean value of HoA are known from satellite observations, can be applied to determine AGB. Identification of reference areas is supposed to be helped by means of satellite estimation of  $q_0$  and maximum height.

It is premature to comment on applications, as further validation under a wider range of forest conditions, than studied so far, is necessary. The availability of a DTM from the BIOMASS mission must be confirmed, and the implications of its 100-m resolution should be evaluated. In addition, the potential for obtaining a high-resolution DTM from Luton-1 should be investigated [42].

### XII. CONCLUSION

The objective of this article has been to demonstrate why the mean value of TanDEM-X phase heights, derived from multiple acquisitions, such as the TanDEM-X World DEM and the Copernicus DEM, corrected using a DTM, is approximately proportional to AGB. To support this, data from the Krycklan and Remningstorp sites, along with ESA ground truth campaigns, have been used. These two sites differ not only in forest conditions and climate but also in terms of microwave properties, such as forest attenuation, the  $\sigma_{\rm gr}^0/\sigma_{\rm veg}^0$ -ratio, and HoA values for the acquisitions studied. As such, they represent a broad range of boreal forest conditions. It was then shown that the mean phase heights from 14 TanDEM-X acquisitions over Krycklan and 18 over Remningstorp correlate with AGB. with  $r^2$  values around 0.9, as well as with the product of vegetation ratio and H95.

Exact and approximate IWCM expressions were derived for the TanDEM-X phase height as a function of height (h), density  $(\eta)$ , HoA, two-way attenuation coefficient  $(\alpha)$  and the backscatter ratio  $(\sigma_{\rm gr}^0/\sigma_{\rm veg}^0)$  of the forest layer. By varying the latter two parameters across their observed ranges using Monte Carlo simulations, a mean expression for TanDEM-X phase height was established. This expression showed an approximate proportionality to the product of height and density  $(h\eta)$ , representing mean canopy height, and also a near-linear proportionality to AGB, modeled as  $ah^b$ , for both study sites, with a certain dependence on HoA.

A mean phase height together with ten percent of the stands for training (as few as possible assumed known) resulted in RMSEr between 10% and 20% for estimated height and RMSEr between 11% and 18% for AGB, depending on training information and site.

As a next step, the World DEM and ICESat  $q_0$  should be investigated, e.g., for the Swedish National Forest Inventory, NFI, areas and other known areas with basic forest information including AGB and DTM, cf. [24] and [30], and if possible, derive a relation between the slope value and some forest property, such as  $q_0$  and max. height, which can be investigated independently by means of satellites.

TanDEM-X for AGB estimation has high resolution, no AGB saturation, and world-wide DEM coverage. However, a DTM is needed, and reference areas or a known AGB allometry to convert height information to AGB. The accuracy of the estimates is likely to be high due to the sensitivity to the forest structure, height as well as density. With the impact of previous and present bistatic InSAR satellites, SRTM, TanDEM-X, and the L-band Luton, we may hope for future X-, C- and even L-band bistatic InSAR observations.

## APPENDIX A TANDEM-X ACQUISITIONS FROM REMNINGSTORP AND KRYCKLAN

#### TABLE VI RELATING TANDEM-X ACQUISITION NUMBER USED IN THIS ARTICLE WITH DATE AND HOA

REMNINGS-	DATE	НоА, м
	DATE	HUA, W
TORP #		
0	20110604	49.092
1	20111123	184.958
2	20111226	178.172
3	20120117	172.224
4	20120128	182.026
5	20120201	79.994
6	20120208	178.978
7	20120212	78.632
8	20120219	185.684
9	20120223	78.889
10	20120301	185.767
11	20120312	187.095
12	20120323	183.043
13	20120528	349.324
14	20120722	338.747
15	20120802	314.876
16	20120813	358.674
17	20120824	301.208

KRYCKLAN #	DATE	Ноа, м
18	20110617	52.048
19	20110720	54.107
20	20110811	55.498
21	20110822	56.352
22	20120225	79.411
23	20120717	36.134
24	20120808	37.490
25	20120819	38.518
26	20130601	49.969
27	20130623	51.672
28	20130726	62.249
29	20131227	135.942
30	20140713	37.57
31	20140826	69.116

### APPENDIX B DEVELOPMENT OF AREA-FILL EXPRESSION

The first expression for the area-fill used together with IWCM was based on measurements using a helicopter born scatterometer to determine how backscatter was related to stem volume [35] but also verified by upward-looking photographs [8]. Since such scatterometer measurements are very rare an area-fill expression

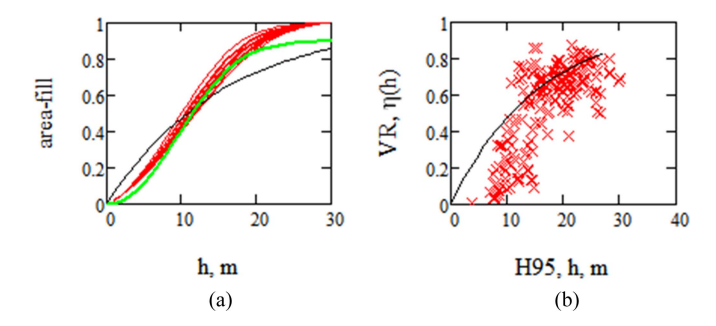


Fig. 14. (a) Illustrating models for area-fill. Expression based on  $\beta$  in red, based on ALS in green, and based on the presently used ICESat expression in black. (b) Illustration of vegetation ratio versus H95 in Remningstorp and the area-fill expression  $\eta(0.065,h)$ .

 $0.9(1-e^{-0.01V})$ , based on local ALS observations, was later used. Now we use an expression  $1-e^{-q0h}$  since a value on q0 can be estimated from ICESat [29]. The value of  $\beta$  was determined by the observations and  $\eta$  will, therefore, vary slightly for the different observations. Looking back at the first solution with IWCM and TanDEM-X observations [9] the area-fill expressions are illustrated in Fig. 14.

### APPENDIX C VEGETATION RATIO AND BASAL AREA

h is a proxy for Lorey's height, hL, in IWCM when in situ data are used, and  $\eta(q0,hL)$  can be seen as a measure of density, which is also the case for basal area, BA. It is known [41] that BA times Lorey's height is proportional to AGB. We find  $0.256 \cdot BA \cdot h = AGB$ , for a data set consisting of 30 plots in Krycklan [25]. However, the relation between VR and BA is nonlinear. We apply a simple one-parameter exponential fit between the gap frequency, 1-VR, and BA, i.e.,  $1-VR = e^{-0.04 \cdot BA}$ , which fulfils the demands when BA is zero and large. This means that  $0.04 \cdot BA = q0 \cdot hL$  and AGB can be expressed as  $7.31 \cdot q0 \cdot hL^2 = 0.402 \cdot hL^2$ . The results are illustrated in Fig. 15.

Data are from Krycklan for which the AGB(H95)-allometry was identified as  $0.28 \cdot \text{H95}^{2.041}$  based on ALS data with hL  $\approx$  H95, and the expressions are approximately the same. The analysis underlines the earlier remarks that the relation between  $\eta(q0,hL)hL$  and AGB is slightly nonlinear. BA1 = q0~hL/0.04 is an approximate expression for basal area based on VR represented as  $\eta(q0,hL)$ , see Fig. 15.

The relations in this Appendix are based on Krycklan-data and due to limited data and a simple approach only indicative of a more general relation between  $\eta(q0,h)$  and basal area for different forest properties/structures.

### APPENDIX D EXACT EXPRESSION FOR IWCM PHASE HEIGHT

We use the law of sines and obtain from Fig. 16

$$\frac{\sin \delta}{M} = \frac{\sin (\varphi - \delta)}{\gamma_{\rm vol}} = \frac{\sin \varphi \cos \delta - \cos \varphi \sin \delta}{\gamma_{\rm vol}} \tag{D1}$$

$$\tan\left(\delta\right) \left(\frac{1}{M} + \frac{\cos\left(\varphi\right)}{\gamma_{\text{vol}}}\right) = \frac{\sin\left(\varphi\right)}{\gamma_{\text{vol}}} \tag{D2}$$

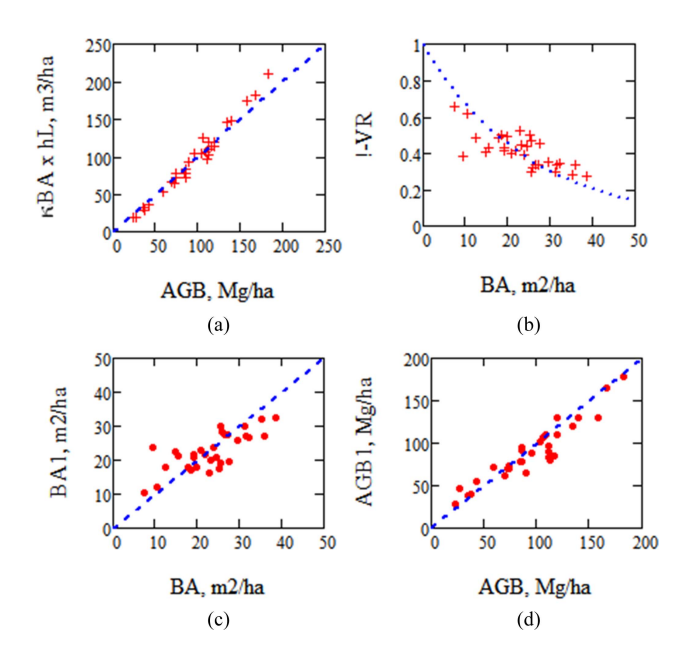


Fig. 15. (a)  $0.256 \cdot \text{BA} \cdot \text{hL}$  versus AGB. (b) Illustrating the gap frequency, 1-VR, versus the basal area for Krycklan and the exponential relation between basal area, BA, in the form  $\exp(\neg 0.04 \cdot \text{BA})$  and 1-VR. (c) BA1 =  $q0 \, hL/0.04$  versus BA, and (d) AGB1 =  $0.256 \cdot \text{BA1} \cdot \text{hL}$  versus AGB.

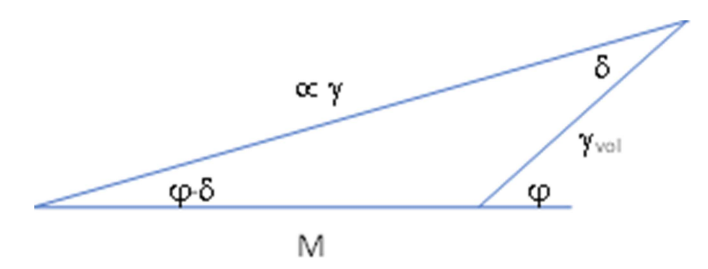


Fig. 16. Illustrating the complex expression  $\hat{\gamma} \propto \tilde{\gamma}_{\rm vol} + M$  with  $\tilde{\gamma}_{\rm vol} = \gamma_{\rm vol} \ e^{-j\varphi} \cdot \varphi - \delta$  is the phase angle of  $\hat{\gamma}$ .

$$\delta = \operatorname{atan}\left(\frac{\sin\left(\varphi\right)}{\left(\frac{\gamma_{\text{vol}}}{M} + \cos\left(\varphi\right)\right)}\right) + n2\pi \tag{D3}$$

PhIWCM = 
$$-\frac{\text{HoA}}{2\pi} \arg(\hat{\gamma}) = -\frac{\text{HoA}}{2\pi} (\varphi - \delta)$$
  
=  $-\frac{\text{HoA}}{2\pi} \left( \varphi - \text{atan} \left( \frac{\sin(\varphi)}{\left( \frac{\gamma_{\text{vol}}}{M} + \cos(\varphi) \right)} \right) + n \cdot 2\pi \right)$ . (D4)

For  $\frac{2\pi}{\alpha \text{HoA}} \ll 1$ ,  $e^{-\alpha h} \ll 1$  we obtain  $\gamma_{\text{vol}} \approx 1$ . The phase height is proportional to  $\arg(e^{-j\varphi} + M)$ , which we can approximate by  $\arg(e^{-j\frac{\varphi}{1+M}})$  when  $M{<}1$  as well as  $M{>}>1$  and with agreement for M=1. From the latter expression we obtain (6) as an approximation for all M.

### ACKNOWLEDGMENT

The author would like to acknowledge L. Ulander and M. Soja for constructive comments. For TanDEM-X data, DLR is gratefully acknowledged and the involved people in the in-situ data made available by ESA for BIOSAR 2008 and 2010. The TanDEM-X acquisitions from Krycklan and Remningstorp were obtained through proposal XT1\_VEG0376 3D Forest Parameter Retrieval from TanDEM-X interferometry.

### REFERENCES

- WMO, "The global observing system for climate: Implementation needs," vol. GCOS-200, ed: GCOS-200, 2016.
- [2] L. Duncanson et al., "Aboveground biomass density models for NASA's global ecosystem dynamics investigation (GEDI) lidar mission," *Remote Sens. Environ.*, vol. 270, 2022, Art. no. 112845.
- [3] M. Santoro et al., "Design and performance of the climate change initiative biomass global retrieval algorithm," Sci. Remote Sens., vol. 10, 2024, Art. no. 100169.
- [4] G. Riegler, S. Hennig, and M. Weber, "WorldDEM-A novel global foundation layer," *Int. Arch. Photogrammetry, Remote Sens. Spatial Inf. Sci.*, vol. XL-3, pp. 183–187, 2015.
- [5] L. M. H. Ulander, J. O. Hagberg, and J. Askne, "ERS-1 SAR interferometry over forested terrain," Eur. Space Agency, vol. 361, pp. 475–475, 1994.
- [6] J. O. Hagberg, L. M. H. Ulander, and J. Askne, "Repeat-pass SAR interferometry over forested terrain," *IEEE Trans. Geosci. Remote Sens.*, vol. 33, no. 2, pp. 331–340, Mar. 1995.
- [7] J. I. Askne, P. B. Dammert, L. M. Ulander, and G. Smith, "C-band repeatpass interferometric SAR observations of the forest," *IEEE Trans. Geosci. Remote Sens.*, vol. 35, no. 1, pp. 25–35, Jan. 1997.
- [8] M. Santoro, J. Askne, G. Smith, and J. E. S. Fransson, "Stem volume retrieval in boreal forests from ERS-1/2 interferometry," *Remote Sens. Environ.*, vol. 81, pp. 19–35, 2002.
- [9] J. I. H. Askne, J. E. S. Fransson, M. Santoro, M. J. Soja, and L. M. H. Ulander, "Model-based biomass estimation of a hemi-boreal forest from multi-temporal TanDEM-X acquisitions," *Remote Sens.*, vol. 5, pp. 5574–5597, 2013
- [10] J. I. H. Askne and M. Santoro, "On the estimation of boreal forest biomass from TanDEM-X data without training samples," *IEEE Geosci. Remote Sens. Lett.*, vol. 12, no. 4, pp. 771–775, Apr. 2015.
- [11] J. I. H. Askne, M. J. Soja, and L. M. H. Ulander, "Biomass estimation in a boreal forest from TanDEM-X data, lidar DTM, and the interferometric water cloud model," *Remote Sens. Environ.*, vol. 196, pp. 265–278, 2017.
- [12] M. J. Soja, J. I. H. Askne, and L. M. H. Ulander, "Estimation of boreal forest properties from TanDEM-X data using inversion of the interferometric water cloud model," *IEEE Geosci. Remote Sens. Lett.*, vol. 14, no. 7, pp. 997–1001, Jul. 2017.
- [13] J. I. H. Askne, H. J. Persson, and L. M. H. Ulander, "Biomass growth from multi-temporal TanDEM-X interferometric synthetic aperture radar observations of a boreal forest site," *Remote Sens.*, vol. 10, 2018, Art. no. 603.
- [14] J. I. H. Askne, H. J. Persson, and L. M. H. Ulander, "On the sensitivity of TanDEM-X-observations to boreal forest structure," *Remote Sens.*, vol. 11, 2019, Art. no. 1644.
- [15] J. Askne and L. M. H. Ulander, "Boreal forest properties from TanDEM-X data using interferometric water cloud model and implications for a bistatic C-band mission," *IEEE J. Sel. Top. Appl. Earth Observ. Remote Sens.*, vol. 14, pp. 8627–8637, 2021.
- [16] S. Solberg, R. Astrup, J. Breidenbach, B. Nilsen, and D. Weydahl, "Monitoring spruce volume and biomass with InSAR data from TanDEM-X," *Remote Sens. Environ.*, vol. 139, pp. 60–67, 2013.
- [17] R. N. Treuhaft and P. R. Siqueira, "The calculated performance of forest structure and biomass estimates from interferometric radar," Waves Random Media, vol. 14, pp. S345–S358, 2004.
- [18] R. Treuhaft et al., "Tropical-Forest Structure and biomass dynamics from TanDEM-X radar interferometry," Forests, vol. 8, 2017, Art. no. 277.
- [19] C. Choi, M. Pardini, M. Heym, and K. P. Papathanassiou, "Improving forest height-to-biomass allometry with structure information: A TanDEM-X study," *IEEE J. Sel. Top. Appl. Earth Observ. Remote Sens.*, vol. 14, pp. 10415–10427, 2021.
- [20] M. J. Soja, H. J. Persson, and L. M. H. Ulander, "Estimation of forest biomass from two-level model inversion of single-pass InSAR data," *IEEE Trans. Geosci. Remote Sens.*, vol. 53, no. 9, pp. 5083–5099, Sep. 2015.
- [21] H. J. Persson, H. Olsson, M. J. Soja, L. M. H. Ulander, and J. E. S. Fransson, "Experiences from large-scale forest mapping of Sweden using TanDEM-X data," *Remote Sens.*, vol. 9, 2017, Art. no. 1253.
- [22] N. Lindgren et al., "Improved prediction of forest variables using data assimilation of interferometric synthetic aperture radar data," Can. J. Remote Sens., vol. 43, pp. 374–383, 2017.
- [23] S. Puliti et al., "Modelling above ground biomass in Tanzanian miombo woodlands using TanDEM-X WorldDEM and field data," *Remote Sens.*, vol. 9, p. 984, 2017.
- [24] M. J. Soja et al., "Sub-hectare resolution forest biomass mapping from Copernicus DEM with low-dimensional models," Sci. Remote Sens., 2025, Art. no. 100250.

- [25] I. Hajnsek, "BIOSAR 2008 technical assistance for the development of airborne SAR and geophysical measurements during the BioSAR 2008 experiment, final report," 2009.
- [26] L. M. H. Ulander et al., "BIOSAR 2010 A SAR campaign in support to the BIOMASS mission," in *Proc. IEEE Int. Geosci. Remote Sens. Symp.*, 2011, pp. 1528–1531.
- [27] L. M. H. Ulander et al., "BIOSAR 2010 technical assistance for the development of airborne SAR and geophysical measurements during the BioSAR 2010 experiment," Final Rep., 2011.
- [28] I. Hajnsek et al., "BIOSAR 2008 technical assistance for the development of airborne SAR and geophysical measurements during the BioSAR 2008 experiment, final report," ESA contract No. 22052/08/NL/CT.
- [29] H. Kay, M. Santoro, O. Cartus, P. Bunting, and R. Lucas, "Exploring the relationship between forest canopy height and canopy density from spaceborne LiDAR observations," *Remote Sens.*, vol. 13, 2021, Art. no. 4961.
- [30] M. Santoro, O. Cartus, and J. E. S. Fransson, "Integration of allometric equations in the water cloud model towards an improved retrieval of forest stem volume with L-band SAR data in Sweden," *Remote Sens. Environ.*, vol. 253, 2021, Art. no. 112235.
- [31] M. Santoro et al., "Retrieval of growing stock volume in boreal forest using hyper-temporal series of Envisat ASAR ScanSAR backscatter measurements," *Remote Sens. Environ.*, vol. 115, pp. 490–507, 2011.
- [32] M. Santoro et al., "Forest growing stock volume of the northern hemisphere: Spatially explicit estimates for 2010 derived from Envisat ASAR," *Remote Sens. Environ.*, vol. 168, pp. 316–334, 2015.
- [33] N. Knapp, R. Fischer, V. Cazcarra-Bes, and A. Huth, "Structure metrics to generalize biomass estimation from LiDAR across forest types from different continents," *Remote Sens. Environ.*, vol. 237, 2020, Art. no. 111597.
- [34] N. Labriere et al., "In situ reference datasets from the TropiSAR and AfriSAR campaigns in support of upcoming spaceborne biomass missions," *IEEE J. Sel. Top. Appl. Earth Observ. Remote Sens.*, vol. 11, no. 10, pp. 3617–3627, Oct. 2018.
- [35] J. T. Pulliainen, K. Heiska, J. Hyyppä, and M. T. Hallikainen, "Backscattering properties of boreal forests at the C-and X-band," *IEEE Trans. Geosci. Remote Sens.*, vol. 32, no. 5, pp. 1041–1050, Sep. 1994.
- [36] G. P. Asner and J. Mascaro, "Mapping tropical forest carbon: Calibrating plot estimates to a simple LiDAR metric," *Remote Sens. Environ.*, vol. 140, pp. 614–624, 2014.
- [37] S. S. Saatchi et al., "Benchmark map of forest carbon stocks in tropical regions across three continents," *Proc. Nat. Acad. Sci.*, vol. 108, pp. 9899–9904, 2011.
- [38] T. Mette, I. Hajnsek, and K. Papathanassiou, "Height-biomass allometry in temperate forests performance accuracy of height-biomass allometry," in *Proc. IEEE Int. Geosci. Remote Sens. Symp.*, 2003, pp. 1942–1944.

- [39] M. Schlund, S. Erasmi, and K. Scipal, "Comparison of aboveground biomass estimation from InSAR and LiDAR canopy height models in tropical forests," *IEEE Geosci. Remote Sens. Lett.*, vol. 17, no. 3, pp. 367–371, Mar. 2020.
- [40] S. Solberg, R. Astrup, T. Gobakken, E. Næsset, and D. J. Weydahl, "Estimating spruce and pine biomass with interferometric X-band SAR," *Remote Sens. Environ.*, vol. 114, pp. 2353–2360, 2010.
- [41] M. Lang et al., "Estimation of above-ground biomass in forest stands from regression on their basal area and height," *Forestry Stud.*, vol. 64, pp. 70–92, 2016.
- [42] Y. Lei et al., "First demonstration of spaceborne L-band bistatic single-polarization single-baseline SAR interferometry on the retrieval of forest vertical structural information," *Remote Sens. Environ.*, vol. 329, 2025, Art. no. 114916.



**Jan I. H. Askne** (Life Fellow, IEEE) was born in Lund, Sweden. He has been active with Chalmers University of Technology, Göteborg, Sweden, in 1961 and a Professor from 1984 to 2001 until retirement.

Prof. Askne has been a Member of the Remote Sensing Committee of the Swedish National Space Board, ESA EOPAG (for ERS-1 and 2), ESA ENVISAT Science Advisory Group on ASAR, and EARSeL committees. He has been involved in a number of international courses on microwave remote sensing and has been the local organizer for

International Symposium on Microwave Signatures in Remote Sensing in 1987, the 14th EARSeL Symposium in 1994, and the ESA ERSEnvisat Symposium 2000, all in Göteborg. He started with projects on wave propagation (in the troposphere, ionosphere, and magnetosphere, plasma, and quantum media) and in radio astronomy (radiation from molecules in cosmic clouds). He shifted in the seventies to work on passive remote sensing (oil spill, meteorological parameters in the troposphere, and ozone in the stratosphere), and later on active remote sensing (sea ice and forestry). Since retirement, his interests have concentrated on interferometric SAR related to forestry. He was the recipient of the Thulin Medal in silver from the Swedish Society of Aeronautics and Astronautics "for important contributions as Scientist and Educator within Swedish and International Remote Sensing," in 2004.